The morphology of poly(aryl-ether-ether-ketone)

D. J. Blundell and B. N. Osborn
Imperial Chemical Industries PLC, Petrochemicals and Plastics Division, PO Box 90, Wilton, Middlesbrough, Cleveland, TS6 8JE, UK
(Received 18 October 1982; revised 25 January 1983)

The morphology and related properties are described for the aromatic thermoplastic poly(aryl-ether-ether-ketone) (PEEK) $[C_6H_4–O–C_6H_4–O–C_6H_4–CO]_n$. Topics covered include crystallinity, crystallization and melting behaviour, lamellar thickness and spherulitic structure. The data are used to derive the following material parameters $T_m^*=395°C$, $\sigma_e=49$ erg cm^{-2}, $\sigma_s=38$ erg cm^{-2} and $\Delta H_F=130$ kJ kg^{-1}. PEEK is closely analogous to poly(ethylene terephthalate) in its crystallization behaviour except that the main transitions occur about 75°C higher.

Keywords Poly(aryl-ether-ether-ketone); crystallization; melting point; crystallinity; lamellae; spherulite

INTRODUCTION

Poly(aryl-ether-ether-ketone) (PEEK) is a tough aromatic polymer with properties which make it very attractive for use as a high-quality engineering thermoplastic. It is a semicrystalline polymer with a crystalline melting point around 335°C and a glass transition at around 145°C. In terms of its thermal properties it is closely analogous to poly(ethylene terephthalate) (PET) with the difference that the main transitions are of the order of 75°C higher – see *Table 1*.

As in the case of PET, PEEK can be quench-cooled from the melt into the glassy state and can therefore be prepared in the crystalline form either by heating up from the glassy state or by cooling down from the melt state. In considering its crystalline morphology it is therefore particularly interesting to make a direct comparison with PET, whose behaviour is more well known.

The crystal unit cell of PEEK has already been discussed in a note by Dawson and Blundell[1] and the synthesis and properties of this class of polymer have been described by Attwood *et al.*[2] These two papers were concerned with the general family of aryl-ether-ketone polymers. In this present paper on crystal morphology and the related crystallization behaviour we will be focusing on the one specific polymer, PEEK, which has the chemical structure:

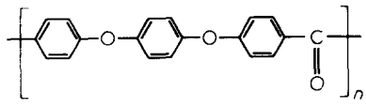

In making comparisons between PEEK and PET, care has been taken to make sure that the PET data have been derived using identical experimental procedures. This is particularly important for material parameters such as the thermodynamic melting point and surface energies, where there is more than one accepted method for determining them. By this means, the comparison between the polymers becomes more self-consistent and any differences are more significant.

EXPERIMENTAL

The PEEK polymers had an intrinsic viscosity (IV) of 1.1 when measured at 25°C in solutions of concentrated H_2SO_4. The comparative PET data were obtained on polymer with IV = 0.65 measured at 25°C in *o*-chlorophenyl solutions.

Densities were measured in a density gradient column made from aqueous solutions of calcium nitrate.

The thermal analysis was carried out with 10 mg samples in a Perkin–Elmer DSC2 which was heated and cooled at 20°C min^{-1}. The DSC2 was linked on-line with a computer to correct the baseline and calibrate the signals.

Wide-angle X-ray diffraction was measured on a Philips vertical goniometer used in the transmission mode.

Small-angle X-ray scattering was recorded with a linear position-sensitive detector on a slit collimated Kratky camera. After background subtraction, the slit smeared intensity $J(s)$ was desmeared and multiplied by the Lorentz factor $4\pi s^2$, to give corrected SAXS curves (where $s=2\sin\theta/\lambda$).

SAMPLE PREPARATION

In order to obtain samples of uniform morphology, attempts were made to crystallize plaques of PEEK isothermally. Two methods were tried.

In the first method, amorphous plaques 1.5 mm thick were made by compression moulding at 400°C for 2 min and then quenching into cold water. The plaques were then rapidly clamped in a press that had been pre-heated to the crystallization temperature T_c, held there for the desired crystallization time t_c and then quenched into cold water.

0032-3861/83/080953-06$03.00

Table 1 Summary of transitions and parameters

	PEEK	PET
T_g (°C)	144	80
T_p (°C)	335	250
T_n (°C) (heating)	180	150
T_c (°C) (cooling)	283	180
T_m* (°C)	395	340
σ_e (erg cm^{-2})	49	93
σ_s (erg cm^{-2})	38	36
ΔH_F (T_p) (kJ kg^{-1})	130	135
ΔS_F (T_p) (kJ kg^{-1} °C^{-1})	0.33	0.40

In the second method, the polymer was melted in a mould at 400°C for 2 min using a small, relatively low mass, temperature-controlled press. The temperature controller was then reset to T_c and at the same time cold air was circulated around the platens of the press to reduce the temperature of the polymer as quickly as possible to T_c. After reaching T_c, the plaque was left for a time t_c before quenching into cold water.

For all these samples, t_c was chosen to be at least five times longer than the time needed to reach the peak crystallization rate (see *Figure 5*). This ensured that the primary crystallization process was substantially complete before the cold water quench. The final quench quickly cools the polymer below the T_g and ensures that no further crystallization occurs after the time t_c.

As will be discussed later, only for some of these samples were we able to achieve reasonable isothermal crystallization without crystallization starting to occur before the sample reached T_c.

RESULTS AND DISCUSSION

Crystallinity and density

Figure 1 illustrates typical wide-angle X-ray diffraction curves for a quenched amorphous sample and for samples of low and high crystallinity. Estimates of crystallinity were obtained by drawing a straight baseline between $2\theta = 10°$ and 36°, and then fitting a scaled amorphous curve under the diffraction peaks in the manner indicated by the broken lines. The ratio of the areas of the crystalline peaks to the total area was taken as a weight fraction index for the X-ray crystallinity, χ.

Figure 2 shows a plot of this crystallinity index against specific volume as measured on a density column. The broken line in *Figure 2* has been drawn from the point for the specific volume of quenched amorphous material (0.792 cm^3 g^{-1}) to a point at 100% crystallinity corresponding to the specific volume of the observed unit cell (0.714 cm^3 g^{-1}). The proximity of the experimental points to this line is an indication of the internal consistency of the density and X-ray index to a two-phase crystalline/amorphous model for this polymer.

Overall crystallization behaviour

Curve A in *Figure 3* shows a d.s.c. trace for a quenched amorphous sample and reveals exactly analogous behaviour to that found with amorphous PET. There is a T_g step at 145°C, followed by an exothermic peak T_n at 180°C associated with crystallization, and then an endothermic peak at 335°C associated with the melting of the crystals. Scans for cooling from the melt at 20°C min^{-1} show a crystallization exotherm T_c at 255°C.

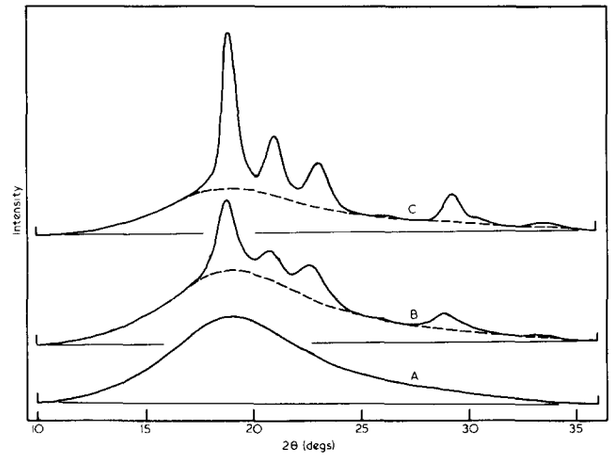

Figure 1 X-ray diffractometer scans for: quenched amorphous sample (curve A); sample crystallized isothermally at 200°C for 1 h (curve B); sample crystallized isothermally at 320°C for 16 h (curve C)

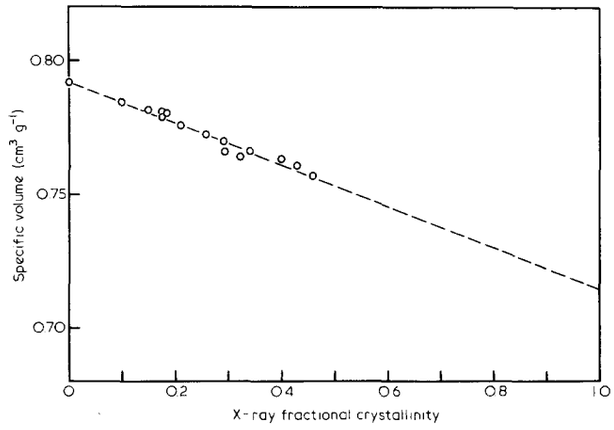

Figure 2 Plot of specific volume *versus* X-ray crystallinity index

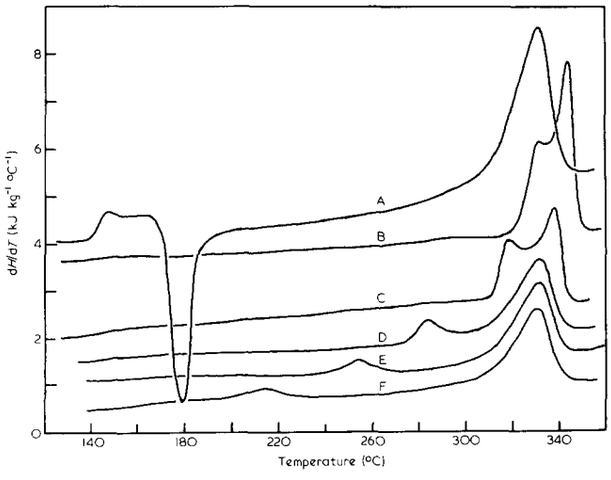

Figure 3 D.s.c. heating scans at 20°C min^{-1} for: amorphous quenched material (curve A); and for samples crystallized isothermally at 320°C for 16 h (curve B); 310°C for 1 h (curve C); 270°C for 1 h (curve D); 230°C for 1 h (curve E); 200°C for 1 h (curve F)

More informative data on the overall crystallization behaviour are given by the isothermal crystallization times t_c shown in *Figure 4*. These data were generated with a Perkin–Elmer DSC2, using two sets of samples. The higher T_c data points were obtained by first melting the polymer at 400°C for 2 min, then cooling rapidly at 320°C min^{-1} down to T_c, and then recording the time at T_c needed for the crystallization process to reach its peak. The lower T_c data points were obtained by first quenching a sample into liquid nitrogen to form the amorphous glassy state, then heating in the DSC2 at 320°C min^{-1} to T_c and then recording the time to reach the crystallization peak. It will be noted that the maximum rate of crystallization for the polymer occurs at around 230°C.

Melting behaviour

Curves B to F in *Figure 3* show d.s.c. heating scans for a series of samples that had been isothermally crystallized at different temperatures. These traces are characterized by two melting processes. There is a smaller, low-temperature process that occurs about 10°C above the crystallization temperature and a larger peak that occurs at a more well defined temperature in the region of 335°C. The precise position of the upper peak depends on the previous crystallization conditions, it being slightly higher for higher T_c.

These observations follow very closely the behaviour of PET and can be explained in terms of the recrystallization phenomenon described by Holdsworth and Turner-Jones[3]. The lower-temperature peak is associated with the melting of crystalline regions formed during the previous isothermal crystallization and as such is characteristic of the melting point of the majority of the crystals present in the d.s.c. sample at room temperature just prior to the heating scan. During the scan above this temperature it is believed that the polymer experiences continuous melting and recrystallization processes. The upper peak represents the point where as a result of the competition between these processes, the net melting rate goes through a maximum, and as such is more characteristic of the polymer system itself. This peak, however, should not be confused with the thermodynamic melting point of an infinitely large crystal, which is discussed later.

Attempts were made to measure the total, net peak area of these melting processes using the approach described by Blundell *et al.*[4] for PET. However, it was found that instrument baseline curvature was not stable enough to give reproducible results for the less crystalline samples. For the higher crystallinity samples which had been crystallized at higher T_c, the temperature spread of the peaks is narrower and reproducible peak areas could be obtained. A comparison between the net peak area and the densities and X-ray index has led us to deduce a heat of fusion ΔH_F of 130 kJ kg^{-1} for fully crystalline PEEK at its melting point. This is similar to the value of 135 kJ kg^{-1} for PET that was deduced by the same procedure.

Lamellar structure

In order to explore the relationship between lamellar structure and T_c, it is essential to have samples that have been crystallized reasonably close to isothermal conditions. Neither of the two groups of sample plaques described in the sample preparation procedure satisfied this requirement over the whole crystallization range. However, by picking selected samples from each group a reasonably consistent set was obtained. The criterion for choosing these samples was based on the appearance of the low-temperature melting process in the d.s.c. scans. Those with ill-defined processes spread over a wide temperature interval were rejected on the grounds that they contained a wide range of crystalline entities. Only those with well defined single low-temperature processes were selected. The chosen samples are listed in *Table 2* and their d.s.c. thermograms are those illustrated as curves B to F in *Figure 3*.

The Bragg long periods of the selected samples deduced from the peaks of corrected SAXS curves are listed in *Table 2*, and show the expected increase with increasing crystallization temperature. Although no direct observation of lamellae has been made in this polymer, it seems reasonable to assume as in other crystalline polymers that the discrete SAXS peaks originate from stacks of lamellae comprising alternate layers of crystalline and amorphous regions. If one assumes that the whole sample is composed of these stacks, then the thickness of the actual crystalline regions, l_c, can be calculated by multiplying the long period by the volume fraction crystallinity ϕ. Values of l_c calculated in this way are listed in *Table 2*.

It will be noted that at the lowest crystalline temperatures, the crystal thickness is only around 20 Å, which is equivalent to a chain sequence of only four phenyl units of 5 Å length. Since the chemical repeat of PEEK comprises three phenyl units[1], one can see that in such small crystals it will be difficult to achieve a representative perfect packing in which the ketone and ether links of neighbouring chains are in perfect register. Instead, we must expect at low T_c that the chains will tend to pack with the ketone and ether links arranged randomly with respect to each other.

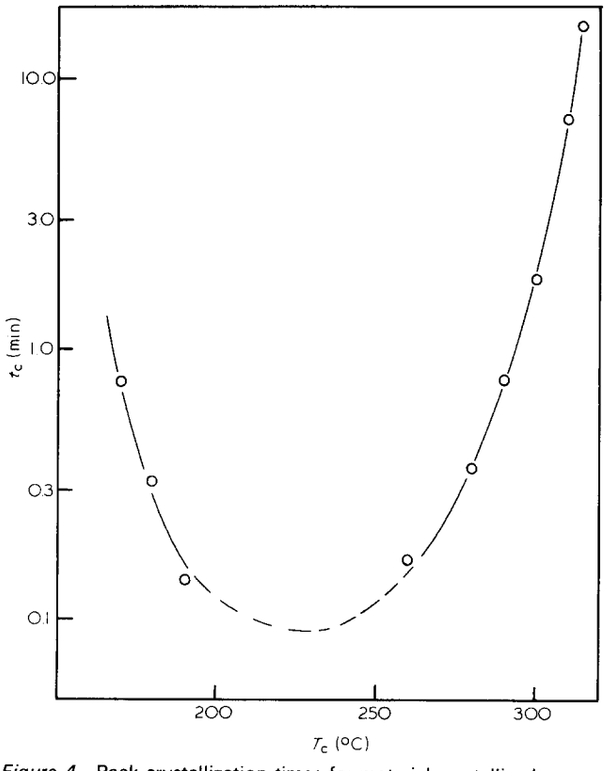

Figure 4 Peak crystallization times for material crystallized isothermally at different T_c

Table 2

	χ (X-ray)	$\phi = \chi\rho/\rho_c$	Long period, d (Å)	$l_c = \phi d$ (Å)	T_L (°C)
Heated to 200°C, 1 h	0.21	0.19	103	20	217
Heated to 230°C, 1 h	0.26	0.24	109	26	254
Heated to 270°C, 1 h	0.29	0.27	121	33	284
Cooled to 310°C, 1 h	0.32	0.30	157	48	320
Cooled to 320°C, 16 h	0.40	0.37	159	59	333

The SAXS data were also calibrated in absolute units in order to obtain the so-called invariant integral:

$$\langle \eta^2 \rangle = 2\pi \int_0^\infty \bar{J}(s) s \, ds$$

If the scatter originates from a two-phase structure with sharp boundaries it is well known that:

$$\langle \eta^2 \rangle = \Delta\rho_e \phi (1 - \phi)$$

where $\Delta\rho_e$ = difference in electron density between phases and ϕ = volume fraction of one of the phases.

By equating ϕ to the measured crystallinity of PEEK, one can use the observed value of $\langle \eta^2 \rangle$ to calculate the effective density difference between the crystalline and amorphous regions. With this procedure our observed invariants were indicating a density difference of 0.14 g ml^{-1} between phases. This agrees reasonably well with the difference between crystallographic unit cell (1.400) and the observed density of amorphous PEEK (1.263) and is therefore further evidence for the validity of the two-phase model for this polymer.

The melting point of the lamellar crystals should be directly related to the crystal thickness l_c by the Thomson–Gibbs equation:

$$T_m = T_m^* \left(1 - \frac{2\sigma_e}{\Delta H_F \rho_c l_c} \right)$$

where T_m^* = thermodynamic melting point of infinite perfect crystals and σ_e = surface energy of planar surface of lamellae.

Following the above discussion on melting processes, the melting point of the crystals which are present in the sample at room temperature, and which are therefore giving rise to the SAXS profiles, should be very close to the observed d.s.c. low-temperature melting process, T_L. *Figure 5* shows a plot of T_L *versus* $1/l_c$. The points lie on a reasonably straight line which extrapolates for $1/l_c \rightarrow 0$ to give an estimate for $T_m^* = 395$°C. This is significantly higher than the final melting peaks in the d.s.c. curves. The slope of this plot yields an estimate for $\sigma_e = 49$ erg cm^{-2}.

It is of interest to compare these results with data for PET, which is a polymer that forms lamellar crystals of similar thickness. Unfortunately the T_m^* and σ_e values in the literature are deduced by a variety of philosophies. In order to be self-consistent in the comparison we will therefore use PET data that have been obtained in our laboratories in an identical manner to that for PEEK. These results are plotted in *Figure 5* for direct comparison. The linear extrapolation gives values of $T_m^* = 340$°C and $\sigma_e = 93$ erg cm^{-2}. The T_m^* value is significantly higher than the normal final d.s.c. melting peaks. It is also much higher than that normally accepted in the literature for the thermodynamic melting point. However, this is no reason to doubt its validity.

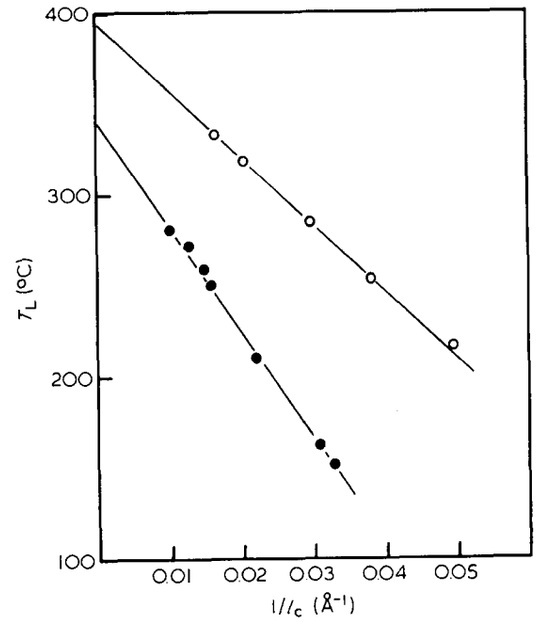

Figure 5 Plot of d.s.c. low-temperature melting process *versus* the reciprocal of lamellar crystal thickness: ○, PEEK; ●, PET

Spherulite morphology

In a polarizing microscope, the standard preparation of PEEK used for the above experiments revealed a complex birefringent mosaic pattern whose scale was too fine to resolve any definite spherulitic texture, indicating that the nucleation density was too high to allow large spherulites to form. However, one special preparation was found with a much lower nucleation density. This material crystallized at a much slower overall rate to give well resolved spherulites when viewed between crossed polarizers. This special sample was therefore used to gather information on the nature and growth rate of spherulites in PEEK.

Small specimens of this material were crystallized isothermally in aluminium pans using a Perkin–Elmer DSC2. The specimens were then sectioned and examined in a polarizing microscope. In this way a direct comparison could be made between the overall growth rate, as monitored by the d.s.c. crystallization times, and the size and number of spherulites as observed microscopically. A typical micrograph from the sections is illustrated in *Figure 6*. All of the spherulites were found to exhibit a positive birefringence.

The size of the spherulites was monitored by measuring the mean chord intercept length, $\bar{L}$, of a random line drawn on the micrographs[5]. Estimates for the mean spherulite radius r were obtained using the very crude approximation that all the spherulites were of identical size, in

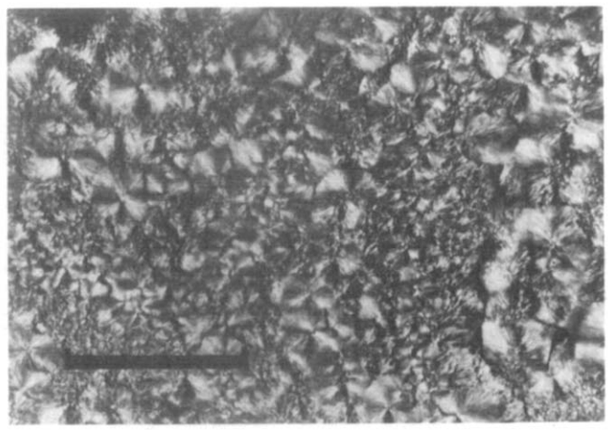

Figure 6 Polarized light micrograph of section cut from sample crystallized isothermally at 287°C. Distance marker=100 μm

which case[5] $r=3\bar{L}/4$. The primary nucleation density of the spherulites was estimated from the relationship

$$N=(4\pi r^3/3)^{-1}$$

These results are tabulated in *Table 3* together with the crystallization times recorded on the d.s.c. Rough values for the linear growth rate of the spherulites were deduced from these data on the basis that the peak crystallization time corresponds to the point where the spherulites impinge. Accordingly, the radial growth rate G will be given approximately by the relationship

$$G=r/t_c$$

It is out of the question to use these approximate data for a detailed analysis of the type of growth mechanism which is occurring. Nevertheless, we believe it is worth while to assume the validity of the well known expression for secondary nucleation and use it as a basis for comparing the behaviour of PEEK with PET. We have therefore fitted the data to the equation that is applicable to regime I kinetics[6]:

$$G=G_0\exp\left(\frac{-4b\sigma_e\sigma_s\ T_m^{*2}}{\Delta H_F\rho_c k\ \Delta TT^2}\right)\exp\left(\frac{-U^*}{R(T-T_g+51.6)}\right)$$

where σ_e = planar surface energy of lamellar crystals, σ_s = side surface energy, b = step height of growth face, and $\Delta T=T_m^*-T$.

Since the PEEK data points are in the region of higher crystallization temperatures where there is minimal suppression from the transport factor, the choice of the transport activation energy U^* is not critical. We have chosen to use a value of $U^*=2000$ cal mol^{-1}. The rate equation can be rewritten in logarithmic form:

$$\log_{10}G+\frac{U^*}{2.3R(T-T_g+51.6)}=\log_{10}G_0-\frac{4b\sigma_s\sigma_e}{2.3\Delta H_F\rho_c k}\frac{T_m^{*2}}{\Delta TT^2}$$

In *Figure 7*, the left-hand side of the equation has been plotted against $T_m^{*2}/\Delta TT^2$. *Figure 7* also shows a similar plot for PET based on the data of Palys and Philips[7] also using $U^*=2000$ cal mol^{-1}. It should be noted that the value of T_m^* used here was 343°C derived from the intercept of our *Figure 5*. It is higher than the value of 280°C used by Palys and Philips in their corresponding plots and results

Table 3 Spherulite growth data

T_c (°C)	t_c (s)	$\bar{L}$ (μm)	N (m^{-3})	r (μm)	G (nm s^{-1})
287	136	29.2	2.3 x 10^{13}	21.9	161
277	71	25.0	3.6	18.75	264
260	28	20.3	6.8	15.2	540
240	13	16.9	11.7	12.7	980

in significantly different slopes from those shown in the plots in their paper.

The raw growth rate data of Palys and Philips is of a higher accuracy and has been obtained with more rigour than our own approximate estimates for PEEK. However, despite these shortcomings in the PEEK data, we believe the difference in slope indicated in the plots in *Figure 7* is probably a genuine and significant effect. Assuming the regime I type kinetics are applicable to both polymers, then these slopes should be given by

$$-4b\sigma_s\sigma_e/2.3k\Delta H_F\rho_c$$

and can thus be used to provide estimates for the side surface energy σ_s. In order to do this, it is necessary to know the thickness b of the monomolecular layer on the growth face. Since we do not yet know which crystallographic plane represents the preferred growth face, we have followed the dictates of the Bravais–Friedel law, which states that the preferred face will be the crystal plane with the largest spacing. In PEEK this plane will be (110), which will give a growth step[1] $b=4.68$ Å. For consistency we have also used the same criterion on the PET data and taken the (010) plane (i.e. $b=5.07$ Å), even though in this case there is some indication from solution-grown crystals that the (100) is preferred[8].

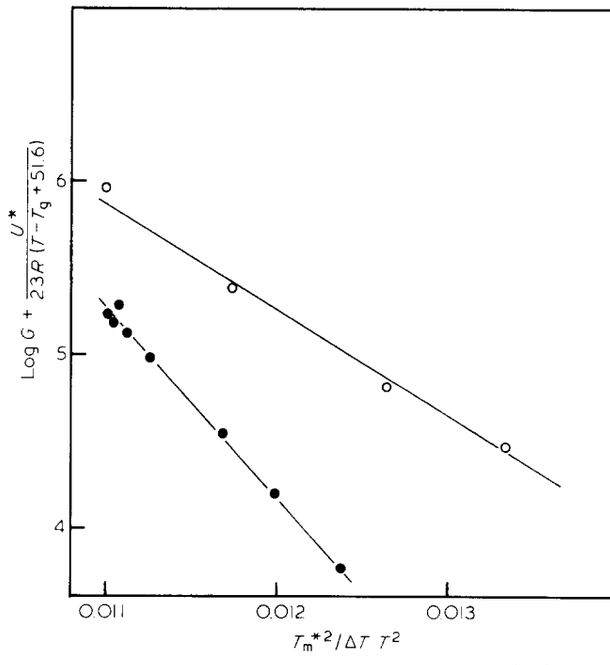

Figure 7 Growth rate data plotted as $\log_{10}G$ *versus* $T_m^{*2}/T^2\Delta T$: ○, PEEK (this work); ●, PET (ref. 7)

These assumptions lead to values for σ_s of about 37 erg cm^{-2} for both polymers. This is higher than is usually encountered with polymer crystals and, in particular, higher than Palys and Philip's value for PET. In the case of PEEK in particular, the results infer that one is approaching the situation where the side surface energy is becoming comparable to the planar surface energy.

CONCLUSION

PEEK fits in well with the generally accepted picture for a crystalline polymer. To a good first approximation, the data are consistent with a two-phase crystal/amorphous structure consisting of crystalline lamellae, whose thickness increases with crystallization temperature. The pattern of thermal transitions closely follows that of PET except that they occur at systematically higher temperatures. The direct comparison with PET of material parameters shows that the main difference is in the planar surface energy σ_e, which is about half of that determined in an analogous way for PET. This indicates a fundamental difference between the polymers in the chain configuration at the crystalline lamellar interface.

REFERENCES

1 Dawson, P. C. and Blundell, D. J. *Polymer* 1980, **21**, 577
2 Attwood, T. E., Dawson, P. C., Freeman, J. L., Hoy, L. R. J., Rose, J. B. and Staniland, P. A. *Polymer* 1981, **22**, 1096
3 Holdsworth, P. J. and Turner-Jones, A. *Polymer* 1971, **12**, 195
4 Blundell, D. J., Beckett, D. R. and Willcocks, P. H. *Polymer* 1981, **22**, 704
5 Underwood, E. E. 'Quantitative Stereology', Addison-Wesley, Reading, Mass., 1970
6 Hoffman, J. D., Davis, G. T. and Lauritzen, J. I. in 'Treatise on Solid State Chemistry', Vol.3 (Ed. N. B. Hannay), Plenum Press, New York, 1976, Ch.7
7 Palys, L. H. and Philips, P. J. *J. Polym. Sci., Polym. Phys. Edn.* 1980, **18**, 829
8 Yamashita, Y. J. *Polym. Sci. A*, 1965, **3**, 81